X-ray Tomograph Measurement of MDT Chambers assembled in Munich

S.Schuh, R.da Silva, R.Voss, V.Zhuravlov

16th January 2006

Contents

Abstract

In this note we present results of the X-ray tomograph measurements of 23 BOS MDT chambers of the ATLAS muon spectrometer assembled at the Max-Planck-Institute for Physics, Munich. The wire positioning accuracy for measured chambers is found to be 17 μm with a spread of 5 μm, 83% of the measured chambers fulfilling the requirement on the wire positioning accuracy of 20 μm. The geometrical parameters of each individual chamber and globally for the production site have been reconstructed. The reinforced and repaired chambers are studied, as well as cut-out chambers.

1 Introduction

The MDT chambers for the ATLAS muon spectrometer require to be assembled with 20 μm accuracy of the signal wire positioning within the chamber [1]. The X-ray tomograph [2] has been constructed at CERN in order to control this stringent requirement. 23 more or less randomly selected chambers out of the series production of 112 BOS chambers assembled at MPI, Munich (24.0%) have been measured by the X-ray tomograph. In addition to those measurements, one chamber prototype [4] and the module 0 [3] have also been measured as part of the production site certification. In this note we did not include the results of the measurements of the prototype and module 0. Table 1 shows the list of measured chambers together with the dates of their production and tomograph measurements.

During the storage of the glued chambers in several cases multilayers were found detached from the spacer structure. In particular, both multilayers of chamber BOS3C06 were completely detached from the spacer, ML1 of chamber BOSXCR3 was completely detached from the spacer, ML1 was detached at the RO end of chambers BOSXCR4 and BOSXAR2, ML1 was detached at the HV end of chamber BOSXCR2. Chambers BOSXCR3, BOS3C06 and BOSXAR2 were re-glued in the production clean room, the other de-touched chambers were repaired in the storage area by gluing an additional aluminum bar at the cross-plate/multilayer joint. In addition to it, a set of chambers were reinforced by similar procedure.

Max-Planck-Institute for Physics produced chambers of BOS type, which have 2 multilayers of 3 layers of MDT tubes of 3900 mm length each. 17 of measured were 72 tubes wide, 3 chambers were 64 tubes wide and one chamber 48 tubes wide.

Chambers BOS6A02 and BOS6A10 have cut-outs at HV end of 12000mm x 14 tubes in both multilayers.

In this note, the counting of the multilayers (ML1 and ML2) is seen as from the ATLAS interaction point (see Fig. 2). The counting of the layers (from 1 to 8) is accordingly, with lower number layers closer to the interaction point.

Each chamber was scanned at five sections as indicated in fig. 1. Sections p1 to p4 were used to measure the alignment platform positions, section p5 was chosen close to the chamber middle. For the cut-out chambers addition section was introduced (p8) close to the end of the short tubes. Typical x-coordinates[1] of the sections are listed in table 2.

Repaired chambers are not included into averaging of geometrical parameters and into the plots withe the parameters distribution.

2 Geometrical parameters

Two-dimensional wire coordinates as measured by the X-ray tomograph were used to determine the geometry of an MDT chamber, which is defined by a grid with the following parameters (see fig. 2):

- z-pitch, the horizontal distance between neighboring wires of the same layer;
- y-pitch, the vertical distance between neighboring layers of the same multilayer;

[1]The chamber coordinate system (see fig. 1) is as following: x-axis is parallel to the chamber wires, y-axis is orthogonal to the layer plane, z-axis is perpendicular to the wires and parallel in the layers planes. The origin is located in the chamber center.

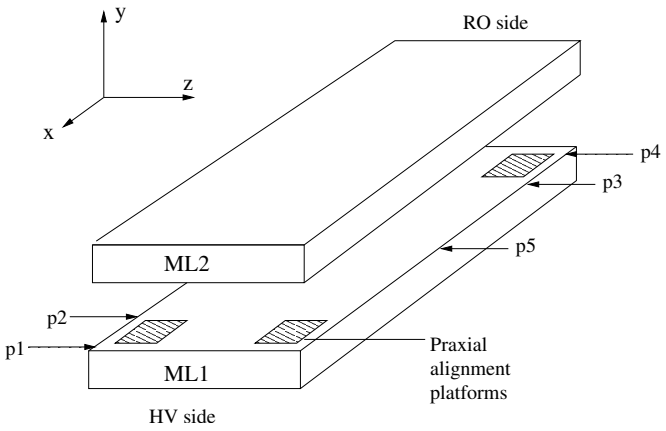

Figure 1: Positions of the scans along the chamber tubes.

- vertical distance between multilayers, dY;
- horizontal shift[2] between multilayers or z-shift, dZ;
- angle between multilayers, dAlpha. [3]

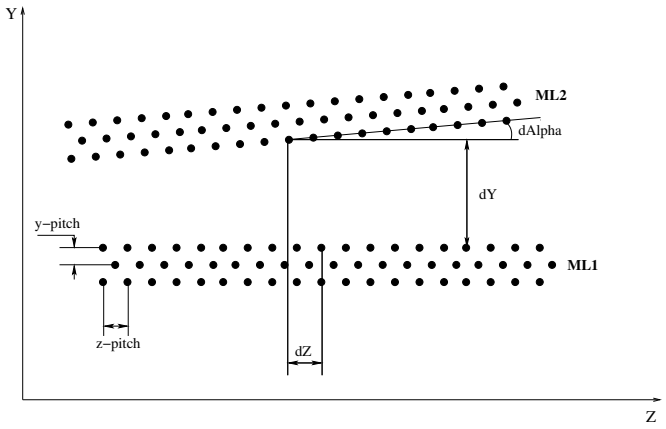

Figure 2: Grid used to determine the geometrical parameters of a chamber; cross-section view from HV end of the chamber.

The chamber geometry parameters were calculated by fitting the grid parameters to the measured wire coordinates of the full chamber. In addition, the following parameters were estimated at the layer level:

- z-pitch of an individual layer;
- vertical distance between layers or interlayer distance;

[2]Z-shift is defined as positive if ML2 is shifted in the direction of z-axis.

[3]The angle between multilayers is defined as positive if ML2 is rotated in counterclockwise direction (view from HV end of a chamber).

- horizontal shift between layers;
- angle between layers;
- sag of a layer derived from a 2-nd order polynomial fit of the wire positions of a layer. Sag of a multilayer is defined from a similar fit of all wires of the multilayer.

In the remainder of this note, we discuss the geometrical parameters derived from sections p6 and p7. Parameters of the section p6 are referred to as "HV end" of a chamber, and parameters of the section p7 are referred to as "RO end".

The nominal values of the grid parameters provided by the production site are listed in table 3. The nominal value for the horizontal shift and angle between multilayers is zero.

The nominal grid is constructed with the nominal geometrical parameters and fitted to the measured coordinates of the wires. The standard deviation of the chamber wires from the fitted grid, considered as a measure of the wire positioning precision, is calculated with the formula

$$\sigma = \sqrt{\frac{\chi^2_{min}}{2 \cdot N - 3}}.$$

Here N is the number of measured wires and χ^2_{min} is the minimal value of the function

$$\chi^2 = \sum (z_i^{meas} - z_i^{grid})^2 + (y_i^{meas} - y_i^{grid})^2.$$

Typical uncertainties on the geometrical parameters are listed in table 4. Systematic uncertainty was estimated by the analysis of the set of 6 scans taken for the same section within short period. Several additional sources of systematic uncertainty were estimated: uncertainty of vertical scale of $2\mu m/m$, tomograph non-orthogonality of $2\mu m/m$ and uncertainty coming from aluminum thermal expansion of 25 $\frac{\mu m}{m \cdot ^\circ C}$. Horizontal scale uncertainty and scale non-uniformity together with single wire measurement accuracy give negligible contribution.

Statistical error is calculated as

$$\sigma_{stat} = \Delta P \sqrt{\frac{\chi^2_{min}}{ndf}},$$

where P is the corresponding geometrical parameter, ΔP is its variation, giving the rise of χ^2 by 1; ndf is the number of degrees of freedom of the fit. The number of wires measured by tomograph in upper multilayer (ML2) is larger than in lower multilayer (ML1), therefore the statistical and systematic uncertainties for the lower multilayer are larger than the the upper one.

3 Results

3.1 Wire positioning precision

Fig.3 shows the the distribution of standard deviation σ and the standard deviation σ as a function of the chamber serial number. 80% of measured chambers are inside the specification of $\sigma < 20$ μm. The average standard deviation is 18.2 μm with 6.0 μm rms. The values of standard deviation σ of all measured BOS chambers are listed in Table 5.

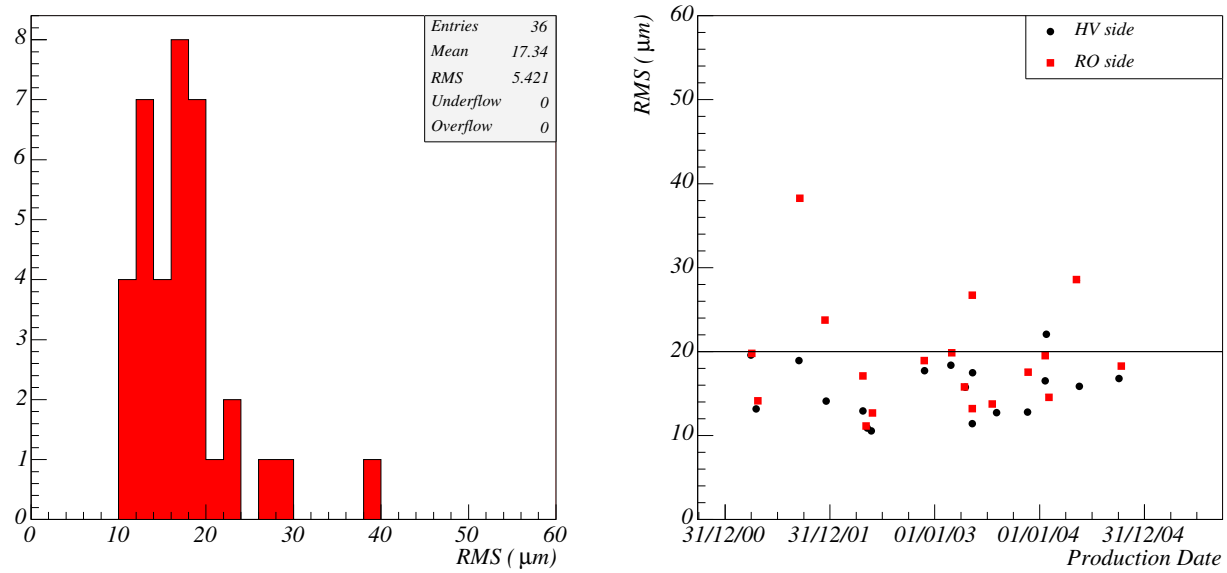

Figure 3: Left: distribution of the standard deviation of BOS chambers from the nominal grid, right: standard deviation as a function of the production date.

3.2 Multilayer parameters

Table 6 gives the z- and y-pitch for all measured BOS chambers for HV and RO ends of the chamber and for ML1 and ML2 separately. Averaged values and RMS are also shown in the table.

Fig. 5 shows the z- and y-pitch plotted versus the production date. For the most of the chambers produced in 2003 and 2004 the z-pitch (fig. 5 left) is below the nominal value of 30.0357 mm. During this period the chambers with 64 and 40 tubes per layers were assembled (narrow chambers), while in 2001 and 2002 the chambers with 72 tubes per layer were produced (wide chambers). For the production of narrow chambers the inner parts of the 72-holdings combs were used. The decrease in z-pitch for narrow chambers with respect to the wide chambers is reflects lower pitch of the inner section of the combs in comparison with outer sections. The z-pitch averaged over all measured BOS chambers were found to be 30035.38 μm with r.m.s. of 0.27 μm. Wide chambers have z-pitch of 30035.45 with r.m.s. of 0.27 μm, and narrow chambers have z-pitch of 30035.25 with r.m.s. of 0.23 μm.

Y-pitch is quite consistent for the whole production period with exception of chamber MPI068, which has y-pitch of ML1 (RO end) 33 μm larger with respect to the nominal one . Vertical geometry of this chamber shown in Fig. 4, where the chamber layers are placed with non-scaled spacing of 100 μm.

The angle between multilayers, multilayer vertical distance and horizontal shift between multilayers are listed in Table 7 together with their average values and RMS. Fig. 6 shows these parameters together with the multilayer sags versus production serial number.

Chamber MPI061 has large shift between multilayers at RO end[4]. Fig 7(left) shows the residual

[4]Actually, the information of RO end, i.e. section p3 is not available for this chamber because the layer recognition failed for this section, we used the section p5 instead. It means that the chamber deformation at RO end is twice larger

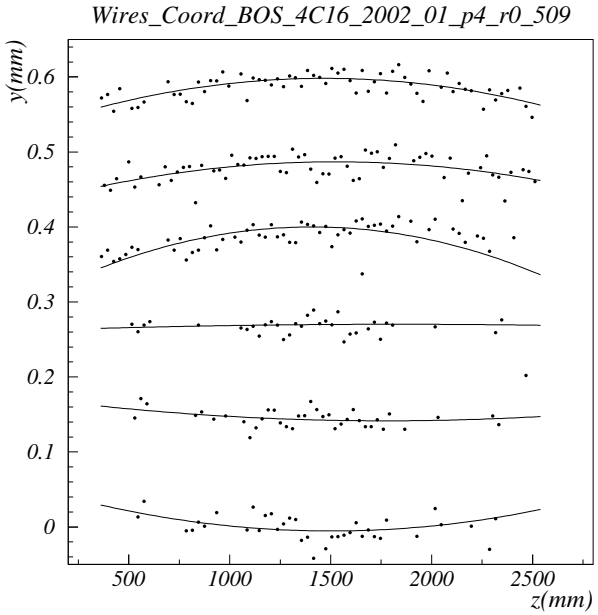

Figure 4: Chamber MPI068, RO end. Wires z-coordinate plotted versus y-coordinate. The nominal distance between layers is reduced to 100 μm.

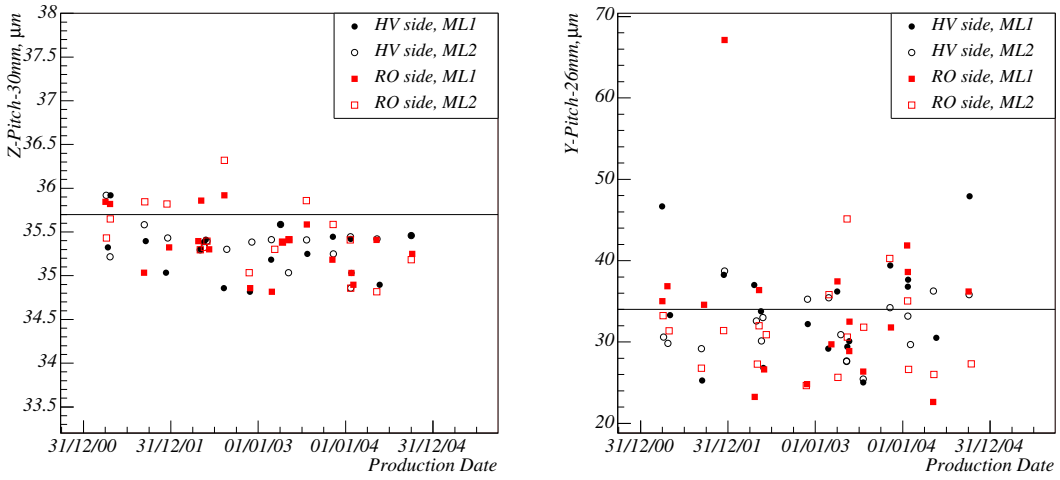

Figure 5: z-pitch (left) and y-pitch (right) as a function of production date. Horizontal lines show the nominal values.

horizontal wire shift versus wire number[5] in the layer. As it can be seen, layers 1 and 2 are shifted with respect to the others by about 100 μm.

than quoted.

[5]Wire numbering goes in the direction of the z-axis.

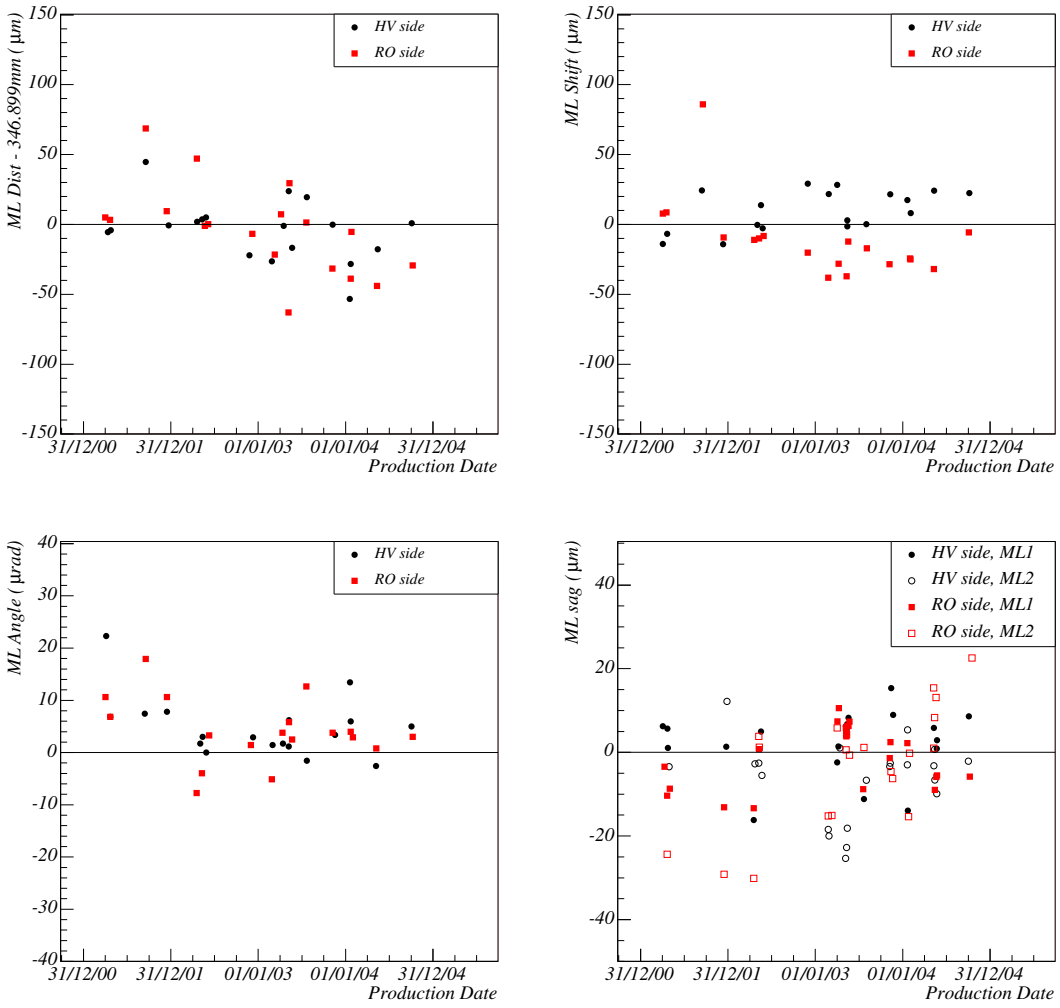

Figure 6: Multilayer distance, multilayer shift, multilayer angle and multilayer sag as a function of production date. Horizontal lines show the nominal values.

4 Reinforced and Repaired Chambers

To insure the mechanical integrity of the chambers some glue joints were reinforces by gluing of an aluminum bar. This bar connected a multilayer with a cross-plate at both ends of the chamber.

X-ray tomograph measured 5 reinforced chambers (see table 1). The aluminum bars used for the reinforcement did not allow to measure section p1 and p4, therefore we describe the HV end of the chamber by the section p2 and the RO end of the chamber by the section p3. These section were taken 232 mm from the ends of the tubes.

No statistically significant deviation were found in the distribution of the reinforced chamber, probably with exception of the distribution of the multilayer shift, which is wider for the reinforced chambers with respect to the distribution of all measured chambers (see fig. 8).

Chambers MPI058, MPI059 and MPI003 were re-glued in the production clean room, chambers MPI062 and MPI065 were repaired at the storage area.

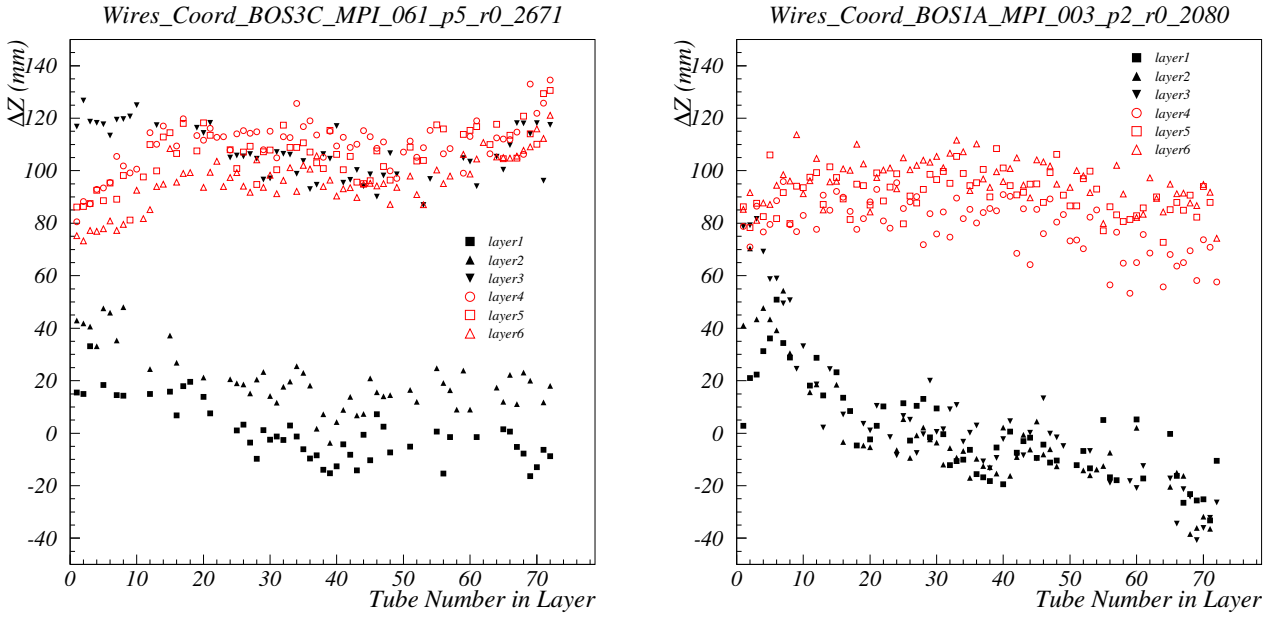

Figure 7: Residual horizontal wire shift plotted versus number of the wire in a layer. Left - chamber MPI061, RO end, right - chamber MPI058, HV end. Both chambers have large multilayer shift.

Chamber MPI058 has a large multilayer shift at HV end. Fig 7(right) shows the residual horizontal wire shift versus wire number in the layer for this chamber. As one can see, in addition to the multilayer shift, this chamber has reduced z-pitch for the ML1, especially for the first 20 wires.

Chamber MPI059 was measured twice, before and after re-gluing. Tables 8 and 9 shows the geometrical parameters of chamber MPI059 before and after re-gluing together with their difference. The observed difference between the first and the second measurements includes the following.

- Decrease of z-pitch of the ML2 by 2.0–2.5 μm. Probably, this is connected with the shrinkage of the glue.
- The significant increase of multilayer distance by 69 μm (HV end) and 91 μm (RO end). The expected increase due to the higher end-pieces used during the gluing was 120 μm.
- ML horizontal shift changed by 93 μm at the HV end and by 141 μm at the RO end.
- Angle between multilayers changed by 26 μrad at the HV end and by 40 μrad at the RO end.

Geometrical parameters for all repaired chambers are summarized in tables 10 and 11. Chamber MPI065 has a bow of 224 μm of the ML2 at the RO end. The right end of the ML2 of the chamber MPI062 is deflected at the HV end by about 200 μm. Chamber MPI003 has a large horizontal shift between multilayers, 124 μm at the RO end and 81 μm at the HV end.

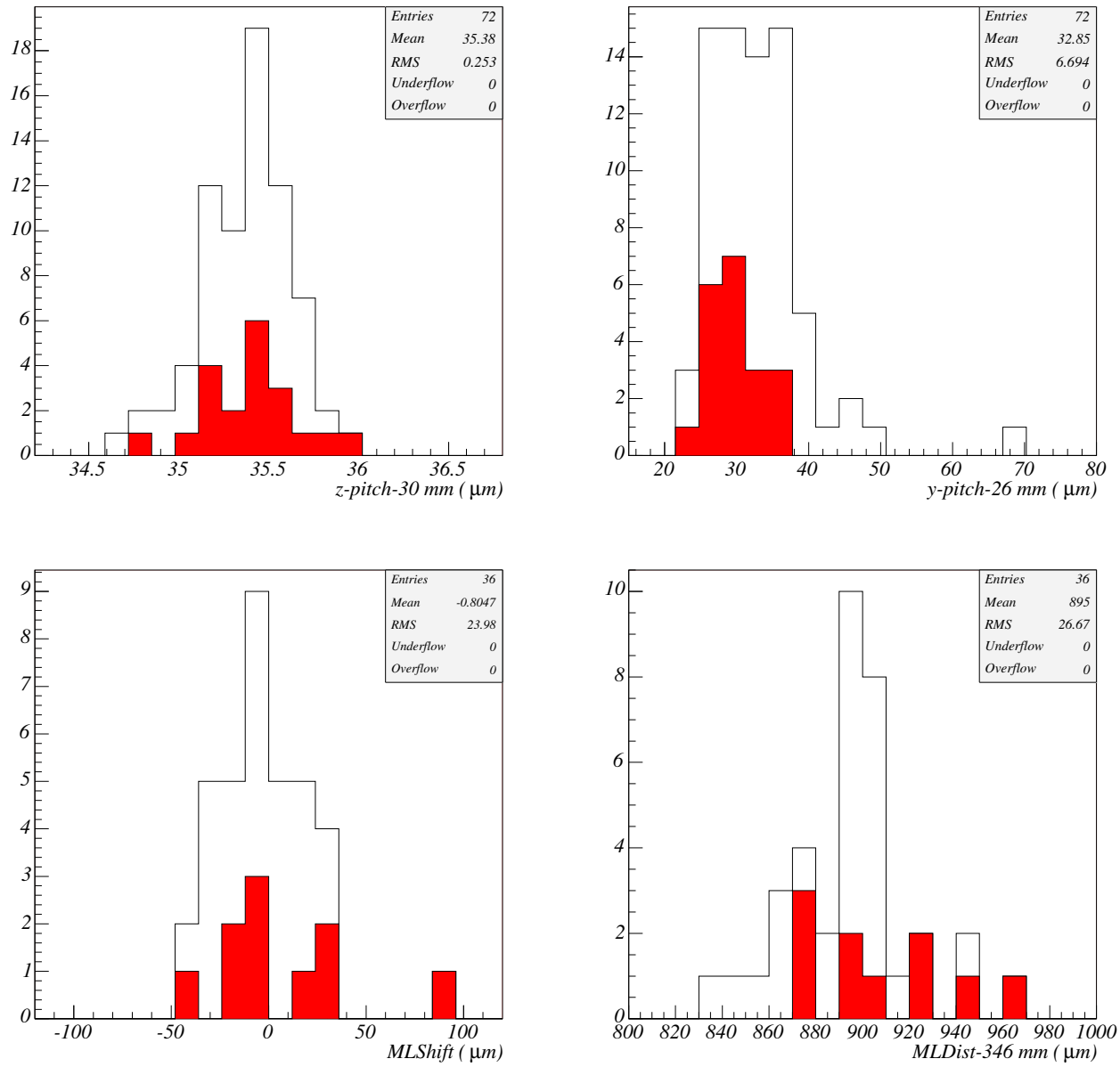

Figure 8: Distribution of the geometrical parameters for BOS chambers. Open histograms show all measured chambers and dashed histograms stand reinforced chambers.

5 Cut-out Chambers

The X-ray tomograph measured two BOS cut-out chambers, MPI031 and MPI033. These chambers have the large cut-outs at both multilayers 1100 mm long and 14 tubes wide. Section p8 (x=746mm) of the chamber MPI031 is shown in Fig. 9, were the residual wire shifts are plotted versus wire number. Cut-out region of the ML1 (wires 30–44) is horizontally shifted by about 50 μm with respect to it nominal value. The cut-out region of the ML2 of the same chamber is also shifted by about 20 μm. The vertical shift of the cut-out region (after appropriate long-beam adjustment) was estimated as

40 μm for ML1 and 20 μm for ML2.

ML2 of the chamber MPI033 is shifted horizontally by about 25 μm, ML1 of this chamber is shifted by about 15 μm vertically, while there were no other significant shifts observed.

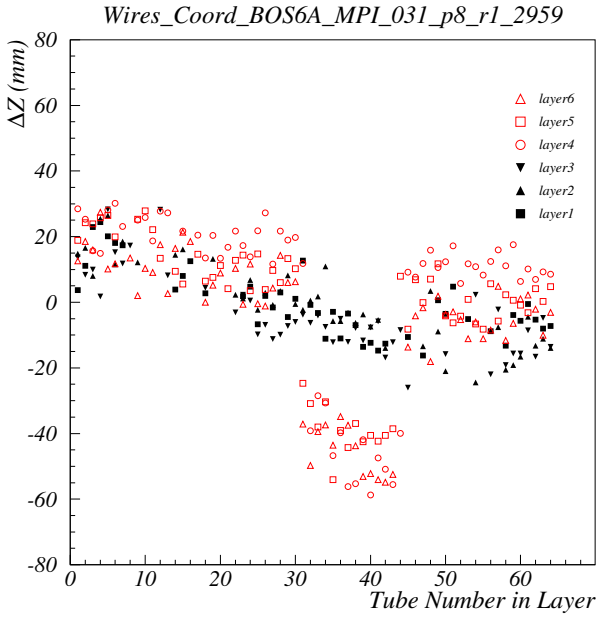

Figure 9: Section p8 of chamber MPI031, measured in flipped orientation (ML2 is above ML1). The residual horizontal shift of the wires s plotted as a function of wire number. Wires with numbers 30–44 of layers 4–6 belong to the cut-out region.

6 Conclusion

A subset of 23 chambers out of 112 chambers produced at Max Planck Institute for Physics in Munich has been measured by the CERN X-ray tomograph. 83% measured chambers fulfilled the ATLAS wire placement specification. New averaged geometrical parameters of the BOS-chambers were derived from the measurements.

The geometry of reinforced chambers was studied and no significant deviation of the geometrical parameters from their nominal values were found. Repaired chambers were found to be with large deviation of multilayer relative position.

Chambers with cut-out were found to have essential shifts of cut-out region.

References

[1] ATLAS Muon Spectrometer Technical Design Report, CERN/LHCC 97-22, 1997.

[2] S. Schuh *et al.,* Nucl.Instrum.Meth.**A518**:73-75,2004.

[3] X-tomograph results for the BOS chamber (August-September 2000) http://cern.ch/xtomo/Results/Munich/Mun_2000_08

[4] Kroha, H; Manz, A; Ostapchuk, A. "Analysis of the X-Ray Tomograph Data of the BOS MDT Prototype Chamber", ATL-MUON-2000-015; Geneva:CERN, 20 Aug 1999

[5] G. Kowarik *et al.*, , "Study of Long-term Geometry Stability of ATLAS Muon Monitored Drift Tube Chambers" Available at http://xtomo.home.cern.ch/xtomo/ComparisonNote_2005.pdf.

Prod. Num.	ATLAS Name	Serial Number	Prod. Date	Meas. Date	width	rein-forced	Comment
005	BOS2C16	MPI054	Apr 2001	Jul 2001	72		
006	BOS2C10	MPI055	Apr 2001	May 2001	72		
012	BOS3C04	MPI061	Sep 2001	Mar 2004	72	yes	
019	BOS4C16	MPI068	Dec 2001	Jan 2002	72		
029	BOS1C10	MPI049	May 2002	Jan 2003	72		
030	BOS1C16	MPI050	May 2002	Jul 2002	72		
032	BOF1C14	MPI082	Jun 2002	Jan 2005	72	yes	
039	BOS2A04	MPI008	Aug 2002	Sep 2003	72	yes	
049	BOS3A16	MPI018	Nov 2002	Dec 2002	72	yes	
057	BOS5A04	MPI026	Mar 2003	Apr 2003	72	yes	
091	BOS1A06	MPI090	Mar 2003	Jun 2003	72		
059	BOS5A08	MPI028	Apr 2003	Nov 2003	72		
064	BOF3A12	MPI039	Jul 2003	Aug 2003	64		
068	BOS1C08	MPI048	Nov 2003	Nov 2003	48		
073	BOF5A14	MPI042	Jan 2004	Feb 2004	48		
074	BOSXAR5	MPI043	Feb 2004	Feb 2004	40		
078	BOS6A02	MPI031	May 2004	May 2004	64		cut-out chamber
080	BOS6A10	MPI033	Oct 2004	Oct 2004	64		cut-out chamber
Repaired chambers							
009	BOSXCR3	MPI058	May 2003	Sep 2003	72	yes	comp. detached ML1
010	BOS3C06	MPI059	Mar 2003	Sep 2001 Mar 2003	72		comp. detached ML1 and ML2
013	BOSXCR2	MPI062	Sep 2001	Sep 2003 Mar 2004	72	yes	ML1 detached at HV end
016	BOSXCR4	MPI065	Nov 2001	Aug 2003 Feb 2004	72	yes	ML1 detached at RO end
035	BOSXAR2	MPI003	May 2003	Sep 2003	72	yes	ML1 detached at RO end

Table 1: List of the chambers measured by X-ray tomograph. The dates of the chamber production and measurements are shown. First column shows the sequential production number while the third column shows reference serial number. 7-th column is the width of the chamber in tubes.

Section	x, mm
p1	1814
p2	1654
p3	-1654
p4	-1814
p5	-200

Table 2: Typical x-coordinates of the tomograph sections.

	May 2001–Jul 2001	Sep 2001–Mar 2003	Apr 2003 - Jan 2005
z-pitch	30.0357	30.0357	30.0357
y-pitch	26.041	26.034	26.034
ML-distance	346.862	347.019	346.899

Table 3: Nominal parameters in mm provided by production site.

Parameter	σ_{scale}	σ_{temp}	σ_{syst}		σ_{stat}		σ_{total}	
			ML1	ML2	ML1	ML2	ML1	ML2
z-pitch, μm		0.2	0.07		0.03		0.2	
y-pitch, μm	0.1	0.2	0.4		0.7		0.8	
ML dist, μm	0.7	2.6	2.2		2.4		4.2	
ML shift, μm	0.7		2.3		1.2		2.7	
ML angle, μRad	0.7		0.6		1.9		2.1	
ML sag, μm					1.0	0.4		
Layer z-pitch, μm		0.2	0.08	0.05	0.06	0.04	0.2	0.2
Layer dist, μm	0.1	0.2	1.4	1.3	2.7	2.2	3.0	2.6
Layer shift, μm	0.1		1.2	0.8	3.5	2.8	3.7	2.9
Layer angle, μRad	0.1		1.2	0.9	3.6	3.0	3.8	3.1
Layer sag, μm					1.7	0.8		

Table 4: Systematical and statistical uncertainty on the geometrical parameters.

Chamber	RMS HV end, *mum*	RMS RO end, *mum*
MPI008	11.9	13.5
MPI018	17.9	18.7
MPI026	18.5	20.2
MPI028	16.1	16.2
MPI031	15.6	28.5
MPI033	16.3	18.0
MPI039	12.9	13.5
MPI042	16.4	14.9
MPI043	22.0	19.7
MPI048	12.8	17.9
MPI049	12.8	17.3
MPI050	11.3	11.0
MPI054	19.7	19.7
MPI055	13.2	14.2
MPI061	18.9	38.4
MPI068	14.3	23.8
MPI082	10.7	13.0
MPI090	17.6	26.6
Repaired chambers		
MPI003	31.4	48.2
MPI058	35.0	20.5
MPI059	47.0	51.8
MPI062	52.0	20.7
MPI065	17.3	98.0

Table 5: Standard deviation of the BOS chambers from the nominal grid.

Serial number	z-pitch (mm)				y-pitch (mm)			
	HV-end		RO-end		HV-end		RO-end	
	ML1	ML2	ML1	ML2	ML1	ML2	ML1	ML2
MPI008	30.0354	30.0356	30.0357	30.0358	26.030	26.028	26.029	26.030
MPI018	30.0352	30.0355	30.0351	30.0351	26.032	26.036	26.025	26.025
MPI026	30.0351	30.0354	30.0352	30.0354	26.029	26.035	26.030	26.036
MPI028	30.0355	30.0355	30.0355	30.0354	26.036	26.031	26.038	26.026
MPI031	30.0351	30.0353	30.0353	30.0352	26.031	26.036	26.022	26.026
MPI033	30.0355	30.0355	30.0355	30.0352	26.048	26.036	26.036	26.027
MPI039	30.0352	30.0354	30.0356	30.0357	26.025	26.025	26.026	26.032
MPI042	30.0353	30.0349	30.0349	30.0352	26.036	26.033	26.038	26.035
MPI043	30.0348	30.0353	30.0350	30.0351	26.039	26.029	26.039	26.027
MPI048	30.0353	30.0353	30.0350	30.0354	26.040	26.034	26.032	26.040
MPI049	30.0354	30.0356	30.0352	30.0356	26.037	26.033	26.024	26.027
MPI050	30.0355	30.0354	30.0356	30.0355	26.034	26.030	26.036	26.032
MPI054	30.0354	30.0356	30.0357	30.0355	26.047	26.031	26.035	26.034
MPI055	30.0358	30.0356	30.0357	30.0357	26.033	26.030	26.037	26.031
MPI061	30.0354	30.0348	30.0348	30.036	26.025	26.029	26.035	26.027
MPI068	30.0351	30.0355	30.0354	30.0357	26.038	26.039	26.067	26.031
MPI082	30.0354	30.0355	30.0353	30.0356	26.027	26.033	26.026	26.031
MPI090	30.0352	30.0350	30.0353	30.0353	26.030	26.028	26.033	26.045
Average	30.0353	30.0354	30.0353	30.0354	26.034	26.032	26.034	26.032
	30.0354				26.033			
RMS	0.0002	0.0002	0.0003	0.0003	0.006	0.003	0.010	0.003
	0.0003				0.007			

Table 6: Z-pitch and y-pitch of all measured chambers, their averaged value and RMS.

Serial number	ML distance (mm)		ML shift (mm)		ML angle (μrad)	
	HV	RO	HV	RO	HV	RO
MPI008	346.923	346.928	-0.001	-0.012	6.1	2.7
MPI018	346.877	346.893	0.029	-0.020	3.1	1.4
MPI026	346.873	346.878	0.022	-0.038	1.5	-4.9
MPI028	346.898	346.906	0.028	-0.028	1.7	4.0
MPI031	346.881	346.855	0.024	-0.032	-2.7	0.5
MPI033	346.900	346.870	0.023	-0.006	4.9	3.0
MPI039	346.918	346.901	0.000	-0.017	-1.3	12.7
MPI042	346.871	346.894	0.017	-0.025	5.8	3.8
MPI043	346.848	346.855	0.008	-0.021	10.3	14.3
MPI048	346.899	346.867	0.022	-0.029	3.5	3.9
MPI049	346.901	346.946	0.000	-0.011	1.6	-7.9
MPI050	346.903	346.898	0.014	-0.010	3.1	-3.7
MPI054	346.894	346.904	-0.014	0.008	22.3	10.5
MPI055	346.895	346.902	-0.007	0.009	7.1	7.1
MPI061	346.943	346.968	0.024	0.086	7.4	17.7
MPI068	346.898	346.909	-0.014	-0.010	7.7	10.7
MPI082	346.904	346.899	-0.003	-0.008	0.1	3.4
MPI090	346.883	346.836	0.003	-0.037	0.9	5.9
Average	346.895	346.895	0.010	-0.011	4.8	4.1
	343.895		-0.001		4.4	
RMS	0.021	0.031	0.014	0.027	5.6	6.1
	0.027		0.024		5.9	

Table 7: ML vertical distance, ML horizontal shift and ML angle of all measured chambers, their averaged value and RMS.

	z-pitch (mm)				y-pitch (mm)			
	HV		RO		HV		RO	
	ML1	ML2	ML1	ML2	ML1	ML2	ML1	ML2
1-st meas.	30.0356	30.0358	30.0358	30.0360	26.026	26.031	26.033	26.031
2-nd meas	30.0358	30.0338	30.0352	30.0335	26.031	26.031	26.032	26.030
Difference	0.0002	-0.0020	-0.0006	-0.0025	0.005	0.000	-0.001	-0.001

Table 8: Geometrical parameters of chamber MPI059 before and after re-gluing: z-pitch and y-pitch.

	ML dist, mm		ML Shift, mm		ML angle, μrad	
	HV	RO	HV	RO	HV	RO
1-st meas.	346.924	346.915	0.016	-0.017	18.6	24.4
2-nd meas	346.993	347.006	0.109	0.124	-7.1	-15.7
Difference	0.069	0.091	0.093	0.141	-25.7	-40.1

Table 9: Geometrical parameters of chamber MPI059 before and after re-gluing: multilayer distance, multilayer shift and multilayer angle.

Serial number	z-pitch (mm)				y-pitch (mm)			
	HV-end		RO-end		HV-end		RO-end	
	ML1	ML2	ML1	ML2	ML1	ML2	ML1	ML2
MPI003	30.0366	30.0358	30.0374	30.0362	26.039	26.037	26.046	26.044
MPI058	30.0348	30.0355	30.0357	30.0364	26.032	26.033	26.040	26.027
MPI059	30.0358	30.0338	30.0352	30.0335	26.031	26.031	26.032	26.030
MPI062	30.0359	30.0351	30.0358	30.0356	26.031	26.021	26.028	26.026
MPI065	30.0355	30.0352	30.0357	30.0352	26.039	26.029	26.039	26.027

Table 10: Z-pitch and y-pitch of repaired measured chambers.

Serial number	ML distance (mm)		ML shift (mm)		ML angle (μrad)	
	HV	RO	HV	RO	HV	RO
MPI003	346.888	346.856	0.081	0.124	-6.5	5.4
MPI058	346.889	346.919	0.092	-0.033	16.5	-27.1
MPI059	346.993	347.006	0.022	-0.038	-7.1	-15.7
MPI062	346.923	346.934	0.030	-0.031	24.6	13.0
MPI065	346.927	347.039	0.025	0.078	23.8	15.6

Table 11: ML vertical distance, ML horizontal shift and ML angle of repaired measured chambers.